Supporting Information (SI)

Highly selective mercury(II) cations detection in mixed/aqueous media by a ferrocene-based fluorescent receptor

María Alfonso,[a] Julia Contreras-García,[b] Arturo Espinosa,[a] Alberto Tárraga,[a]* and Pedro Molina[a]*

[a] *Departamento de Química Orgánica. Facultad de Química. Universidad de Murcia. Campus de Espinardo, E-30100 Murcia, Spain.*

E-mail: pmolina@um.es; atarraga@um.es

[b]*Laboratoire de Chimie Théorique, Université Pierre et Marie Curie, 75005 Paris, France*

Table of contents

2-Ferrocenyl-3*H*-imidazo[4,5-h]phenanthro[4,5-abc]phenazine (3):

^{1}H NMR (400 MHz, DMF-d_7)

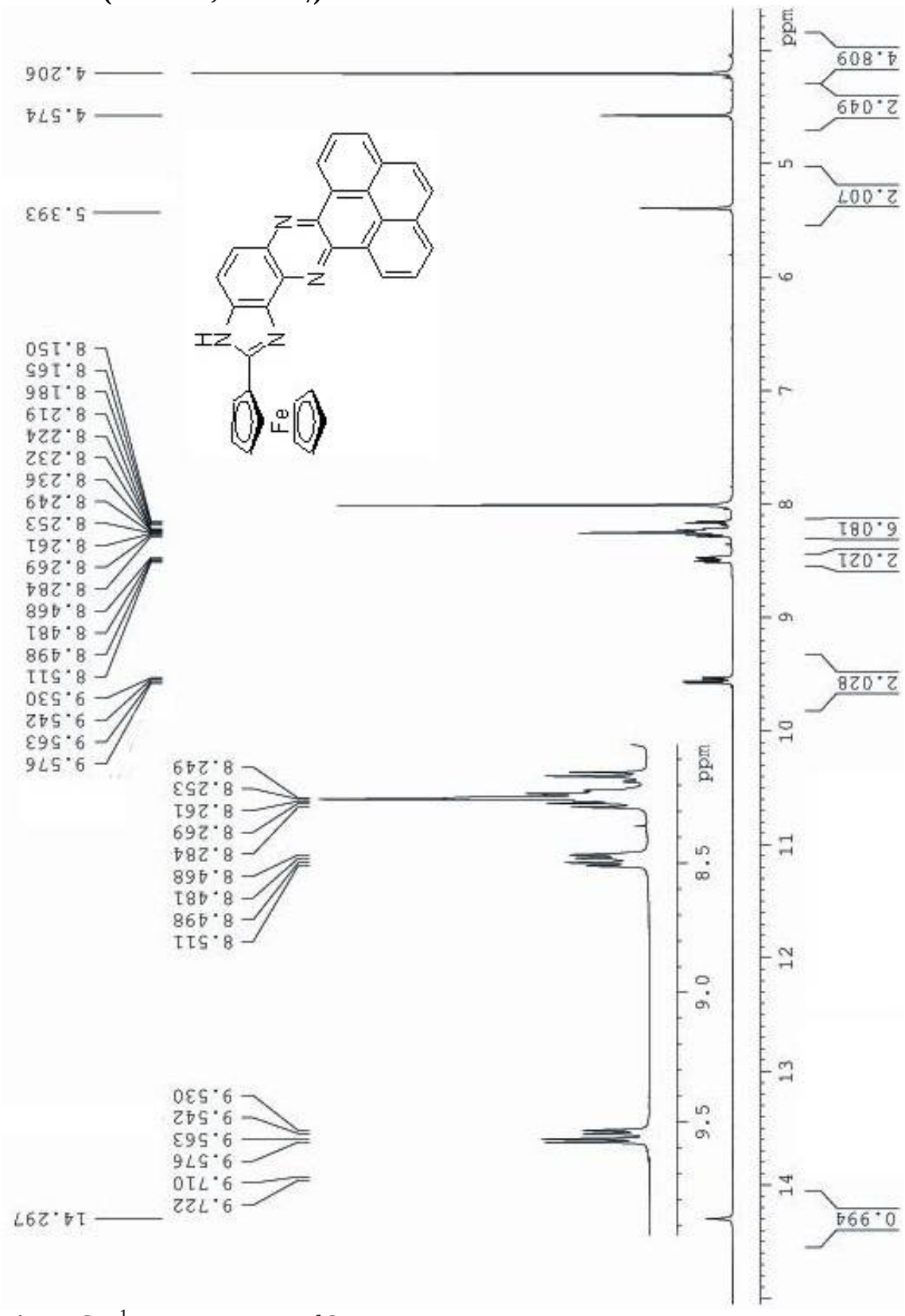

Figure S1. ^{1}H NMR spectra of **3**.

^{13}C NMR (100 MHz, DMF-d_7)

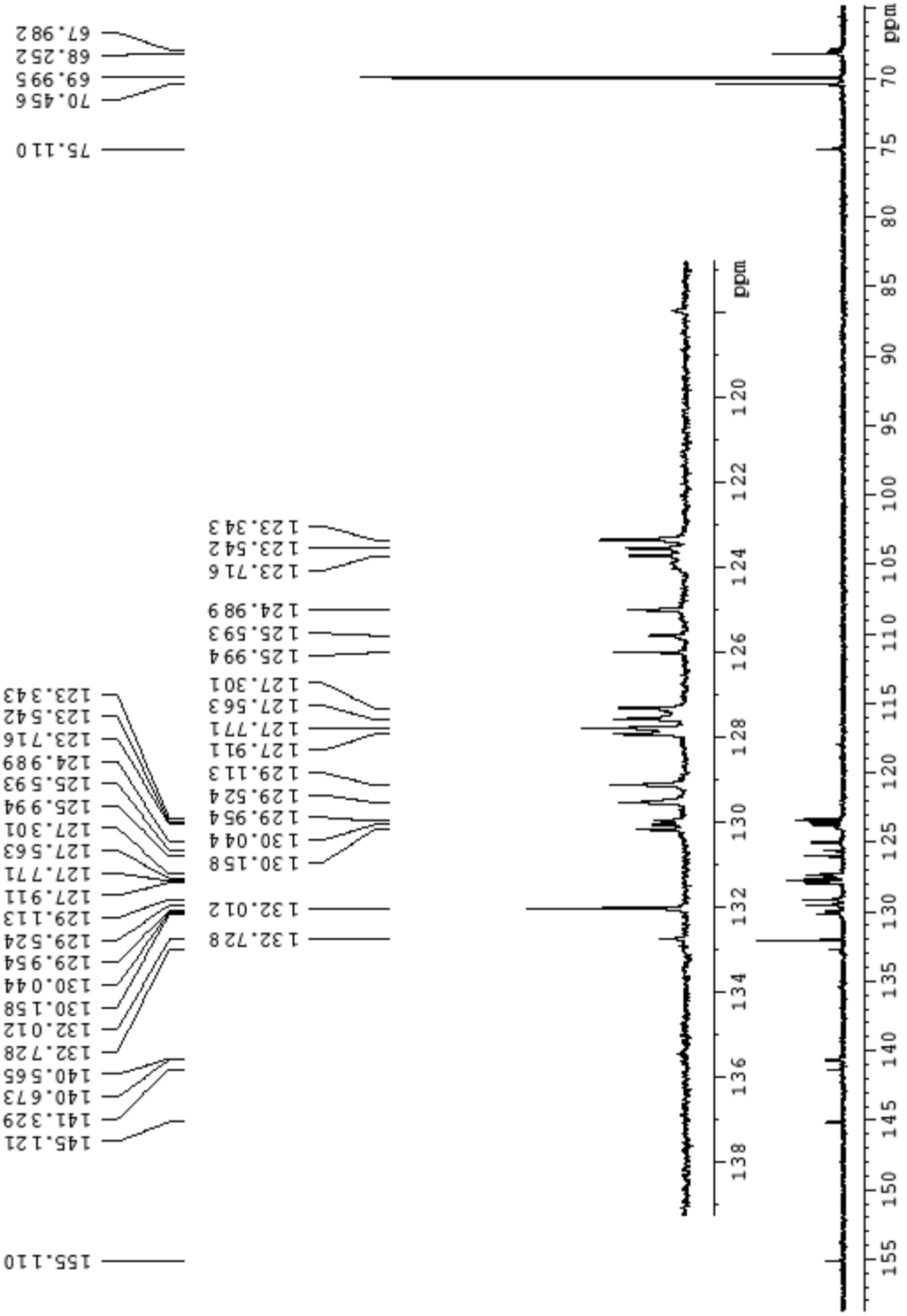

Figure S2. ^{13}C NMR spectra of **3**.

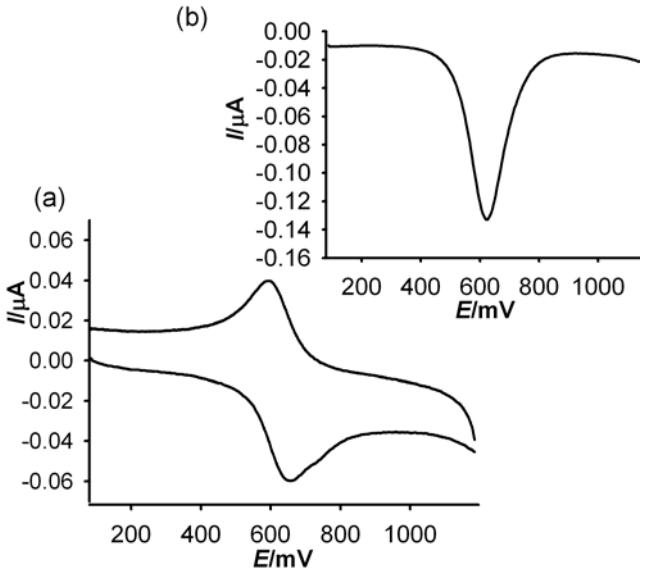

Figure S3. CV (a) and OSWV (b) of **3** ($1x10^{-4}$ M) in CH_3CN using $[(n\text{-}Bu)_4N]PF_6$ as supporting electrolyte.

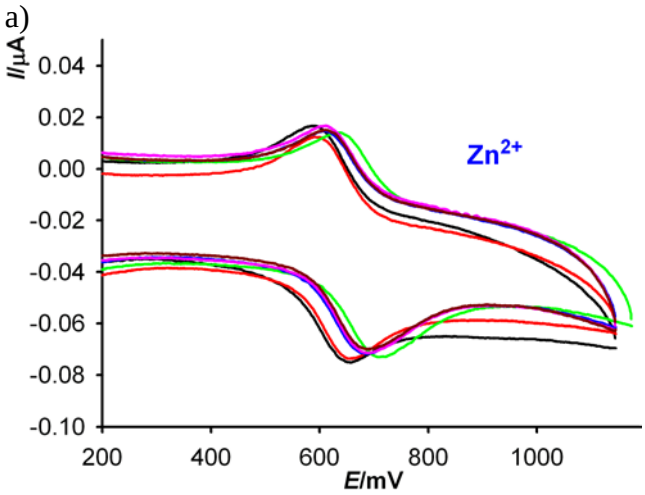

Figure S4. Evolution of the CV of **3** ($1x10^{-4}$ M) in CH_3CN in the presence of increasing amounts of Zn $(OTf)_2$ using $[(n\text{-}Bu)_4N]PF_6$ as supporting electrolyte.

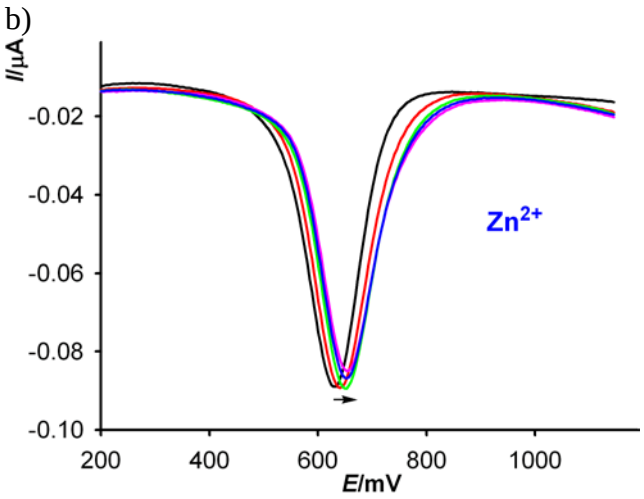

Figure S5. Evolution of the OSWC of **3** ($1x10^{-4}$ M) in CH_3CN in the presence of increasing amounts of Zn $(OTf)_2$ using $[(n\text{-}Bu)_4N]PF_6$ as supporting electrolyte.

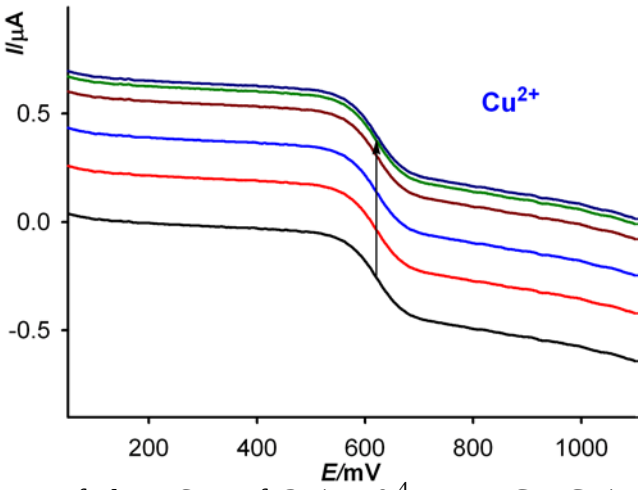

Figure S6. Evolution of the LSW of **3** ($1x10^{-4}$ M in CH_3CN) in the presence of increasing amounts of $Cu(OTf)_2$ obtained by using a rotating disk electrode at 100 mVs^{-1} and 1000 rpm and $[(n\text{-}Bu)_4N]PF_6$ 0.1 M as supporting electrolyte.

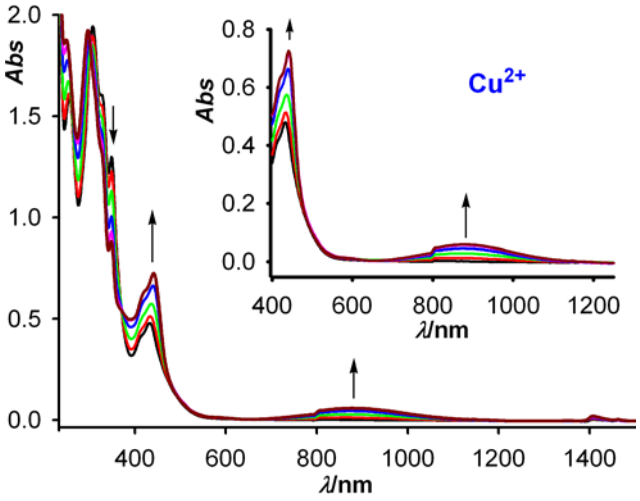

Figure S7. Changes in the absorption spectra of **3** (c = 5 x 10^{-5} M in CH_3CN) upon addition of increasing amounts of $Cu(OTf)_2$, from 0 (black) to 1 equiv (deep red). Arrows indicate absorptions that increase or decrease during the experiment.

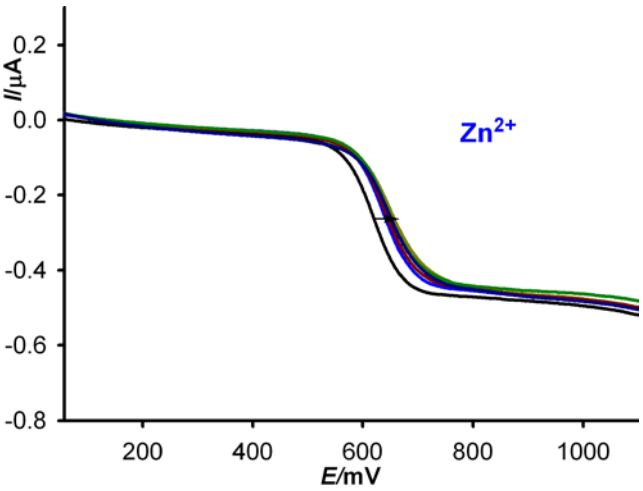

Figure S8. Evolution of the LSW of **3** (1x10^{-4} M in CH_3CN) in the presence of increasing amounts of Zn $(OTf)_2$ obtained by using a rotating disk electrode at 100 mVs^{-1} and 1000 rpm and $[(n\text{-}Bu)_4N]PF_6$ 0.1 M as supporting electrolyte.

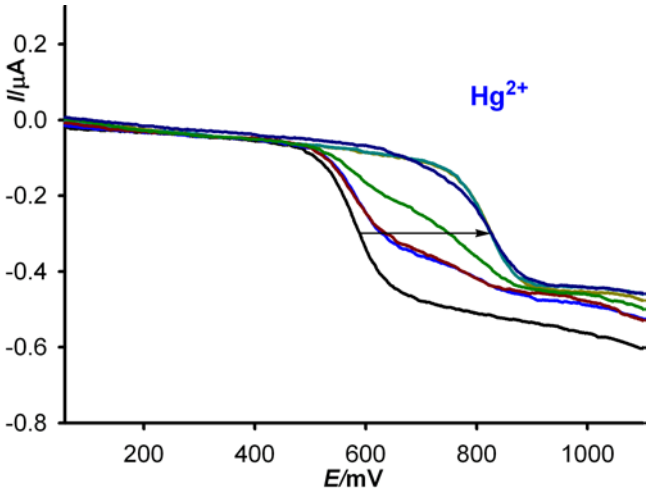

Figure S9. Evolution of the LSW of **3** ($1x10^{-4}$ M in CH_3CN) in the presence of increasing amounts of $Hg(OTf)_2$ obtained by using a rotating disk electrode at 100 mVs^{-1} and 1000 rpm and $[(n\text{-}Bu)_4N]PF_6$ 0.1 M as supporting electrolyte.

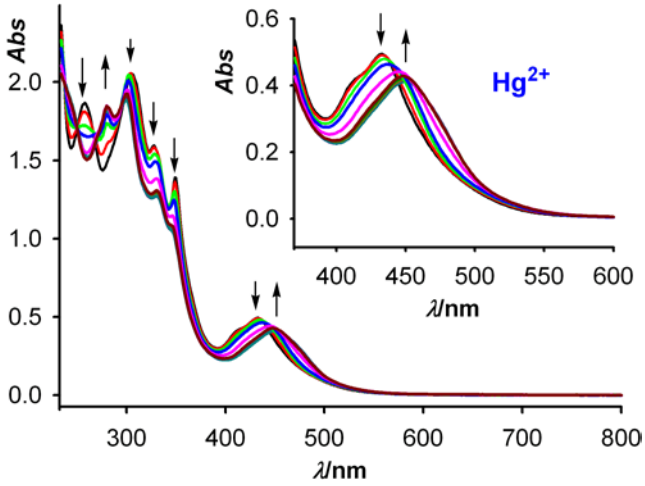

Figure S10. Changes in the absorption spectra of **3** ($c = 5 \times 10^{-5}$ M in CH_3CN) upon addition of increasing amounts of $Hg(OTf)_2$, from 0 (black) to 0.5 equiv (deep red). Arrows indicate absorptions that increase or decrease during the experiment.

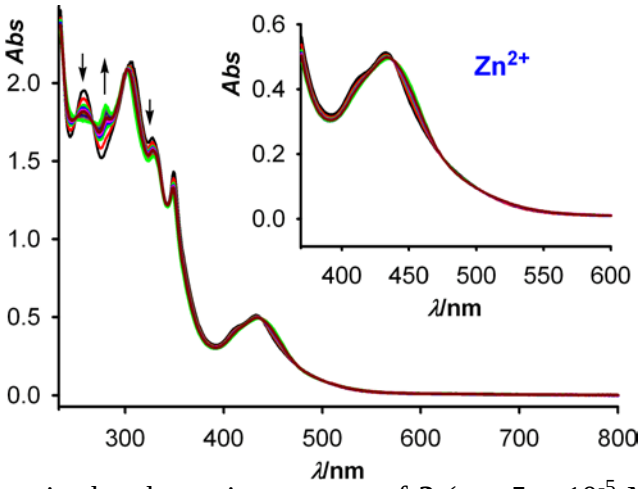

Figure S11. Changes in the absorption spectra of **3** (c = 5 x 10^{-5} M in CH_3CN) upon addition of increasing amounts of $Zn(OTf)_2$, from 0 (black) to 1.0 equiv (deep red). Arrows indicate absorptions that increase or decrease during the experiment.

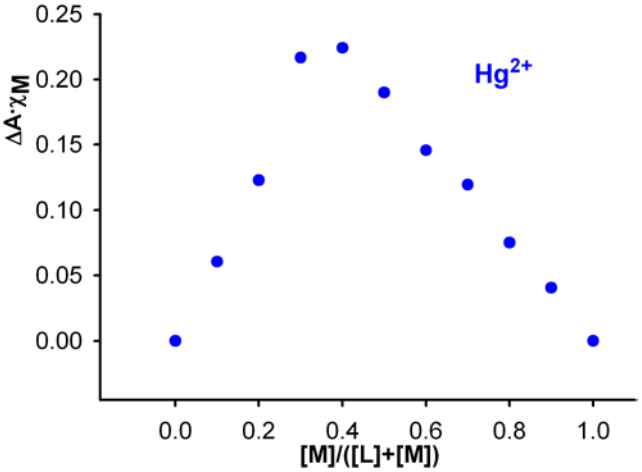

Figure S12. Job's plot for **3** [c = 1 x 10^{-3} M in CH_3CN] and $Hg(OTf)_2$ [0.1 mM in CH_3CN], indicating the formation of a 2:1 complex.

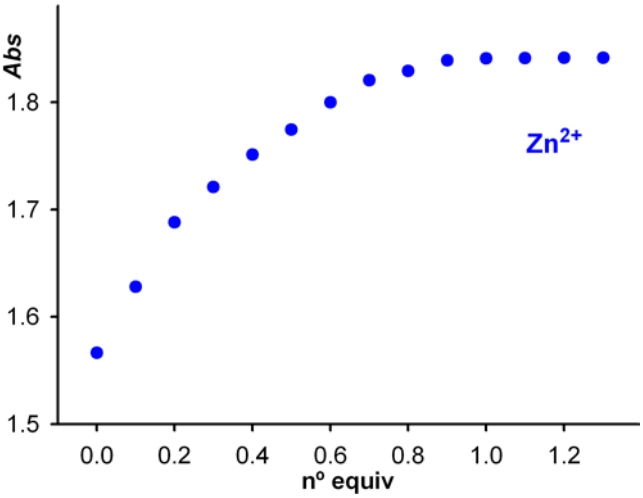

Figure S113. Titration profile showing the absorbance change as a function of the equivalents of $Zn(OTf)_2$ added.

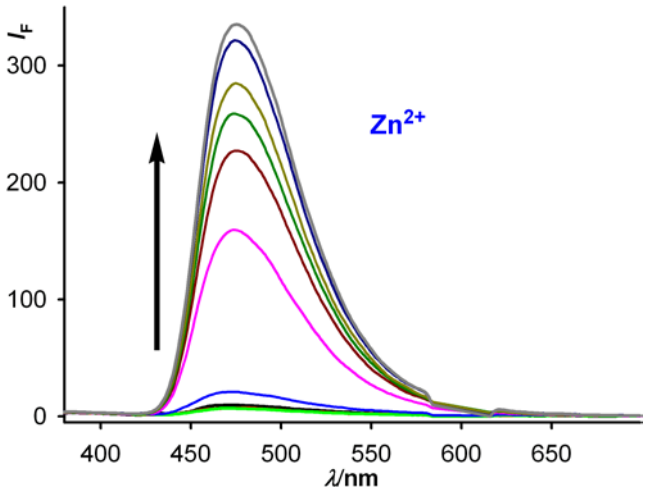

Figure S14. Changes in the fluorescence emission spectrum of **3** (c = 1 x 10^{-5} M) in CH_3CN upon titration with $Zn(OTf)_2$: the initial (black) is that of **3** and the final one (deep gray), after addition of 1 equiv of $Zn(OTf)_2$ (c = 1 x 10^{-2} M in CH_3CN). Emission is monitored at λ_{exc} = 300 nm.

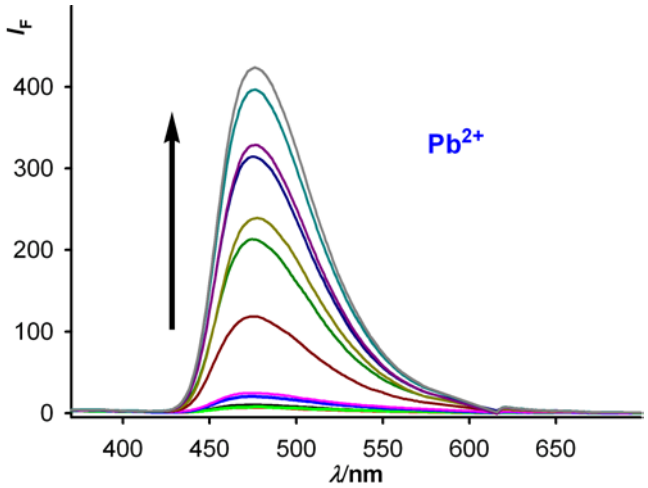

Figure S15. Changes in the fluorescence emission spectrum of **3** (c = 1 x 10^{-5} M) in CH_3CN upon titration with $Pb(ClO_4)_2$: the initial (black) is that of **3** and the final one (deep gray), after addition of 1 equiv of $Pb(ClO_4)_2$ (c = 1 x 10^{-2} M in CH_3CN). Emission is monitored at λ_{exc} = 300 nm.

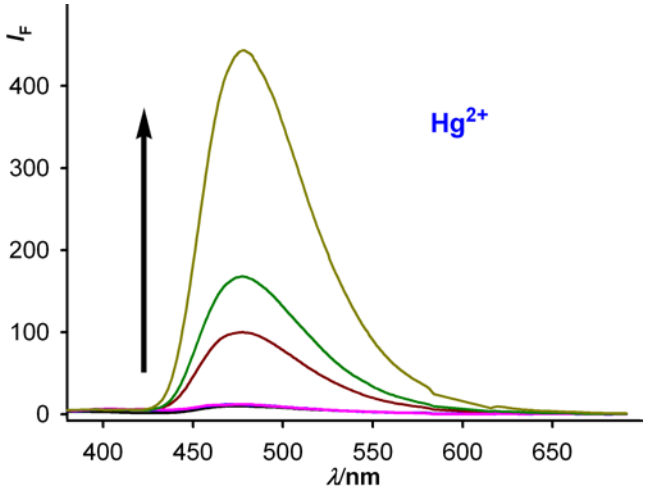

Figure S16. Changes in the fluorescence emission spectrum of **3** (c = 1 x 10^{-5} M) in CH_3CN upon titration with $Hg(OTf)_2$: the initial (black) is that of **3** and the final one (deep yellow), after addition of 0.5 equiv of $Hg(OTf)_2$ (c = 1 x 10^{-2} M in CH_3CN). Emission is monitored at λ_{exc} = 300 nm.

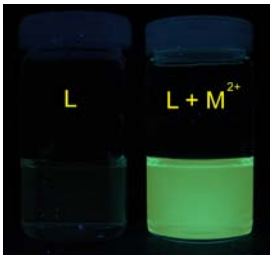

Figure S17. Visual changes observed in the fluorescence of CH_3CN solution of **3** (left) after addition of the cations (right).

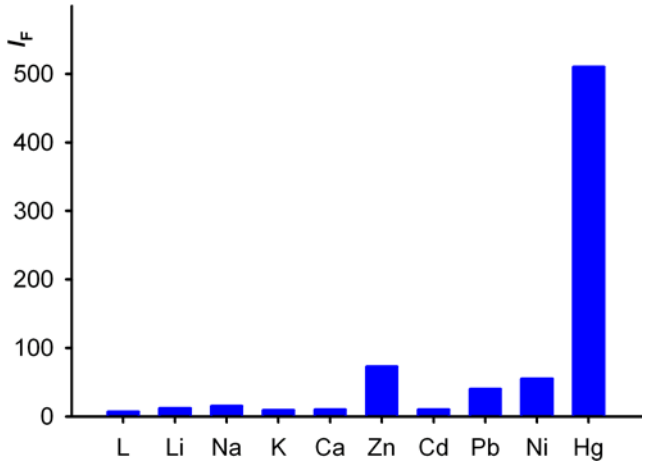

Figure S18. Fluorescence intensity of ligand **3** in CH_3CN/EtOH (70/30), after addition of 1 equiv. of several metal cations. Emission monitored at λ_{exc} = 300 nm.

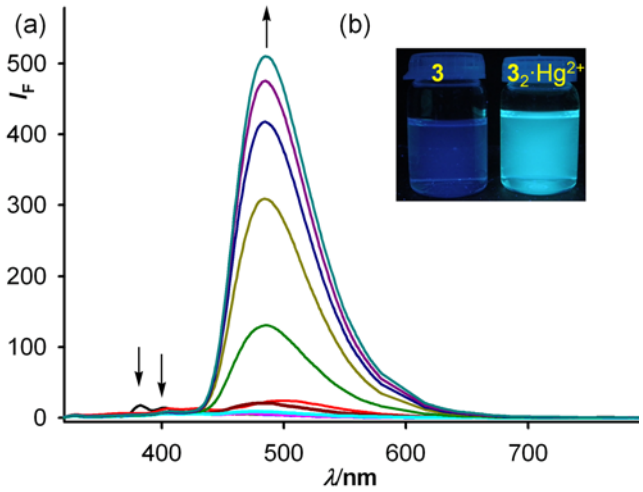

Figure S19. (a) Changes in the fluorescence emission spectrum of **3** (c = 1x10^{-5} M in CH_3CN/EtOH (70/30)) upon titration with $Hg(OTf)_2$: the initial (black) is that of **3** and the final one (deep cyan), after addition of 0.5 equiv. of $Hg(OTf)_2$ (c = 1x10^{-2} M in CH_3CN). Emission is monitored at λ_{exc} = 300 nm. (b) Visual changes observed in the fluorescence of CH_3CN/EtOH (70/30) solutions of **3** (left) and after addition of $Hg(OTf)_2$ (right).

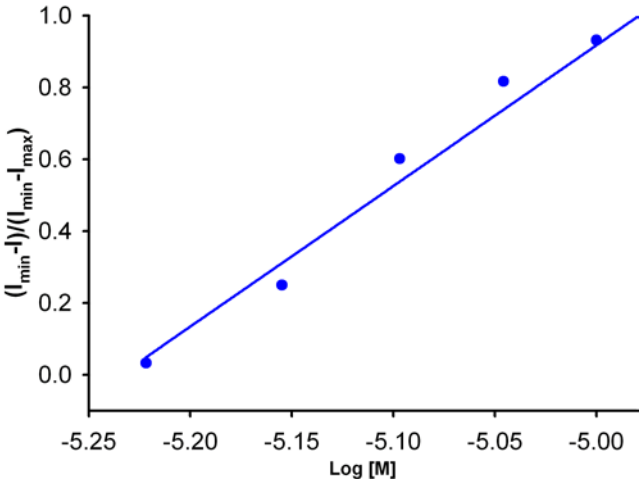

Figure S20. Fluorescence intensity of **3** (c = 1·10^{-4}M in CH_3CN/EtOH (70/30)) at each concentration of $Hg(OTf)_2$ added, normalized between the minimum fluorescence intensity, found at zero equiv of metal cation, and the maximum fluorescence intensity, found at [Hg^{2+}]= 4.10 ppm.

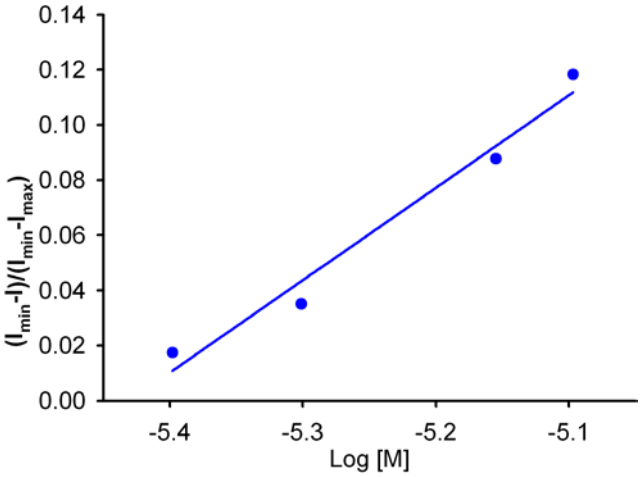

Figure S21. Fluorescence intensity of **3** ($c = 1 \cdot 10^{-4}$M in $CH_3CN/EtOH/H_2O$ (65/25/10) at each concentration of $Hg(OTf)_2$ added, normalized between the minimum fluorescence intensity, found at zero equiv of metal cation, and the maximum fluorescence intensity, found at $[Hg^{2+}]$= 1.52 ppm.

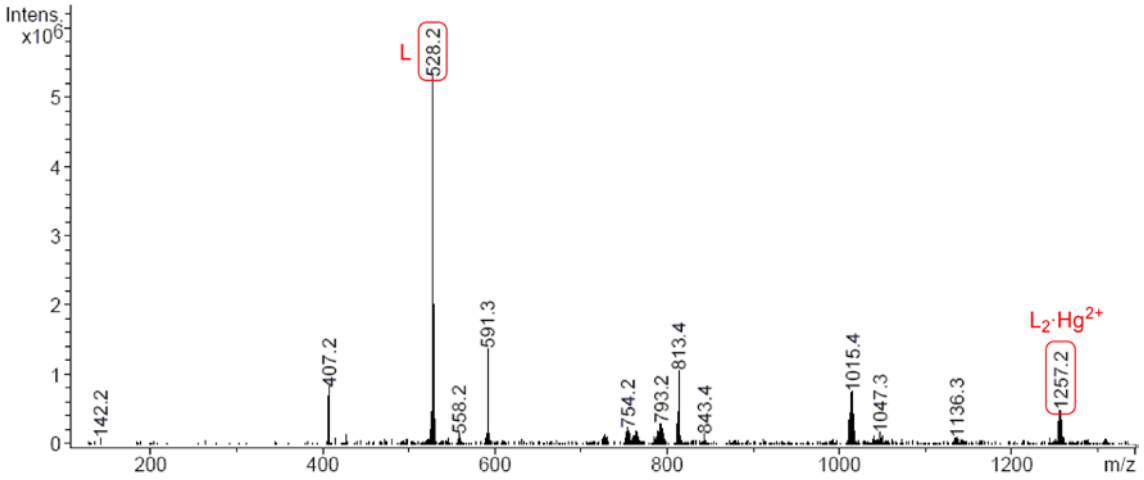

Figure S22. ESI-MS spectra of a $CH_3CN/EtOH$ (70/30) solution of an equimolecular amount of $Hg(OTf)_2$ and ligand **3**.

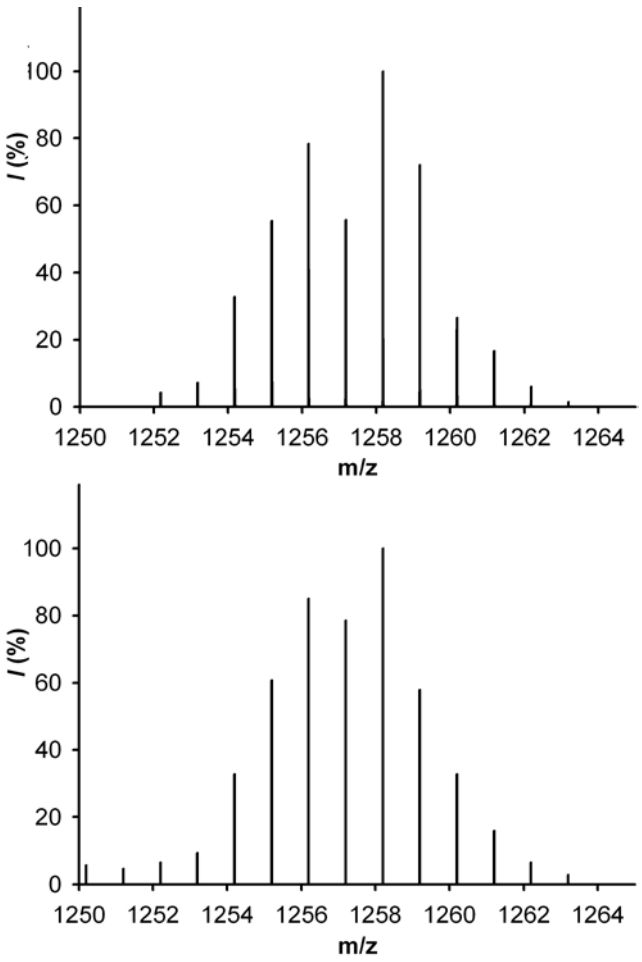

Figure S23. Relative abundance of the isotopic cluster for $\mathbf{3}_2 \cdot Hg^{2+}$ (top) simulated; (bottom) experimental.

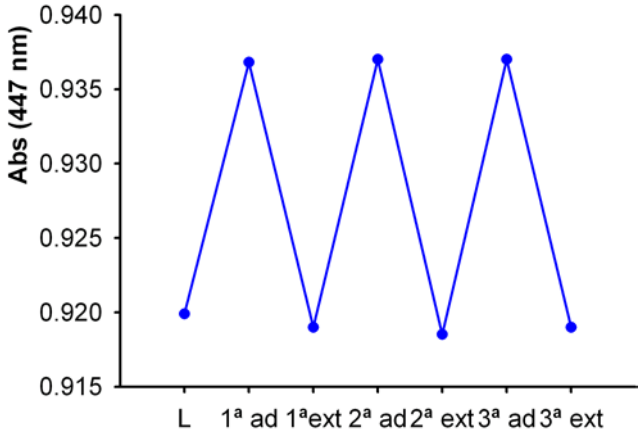

Figure S24. Stepwise complexation/decomplexation (extraction with H_2O) cycles of ligand **3** ($c = 1 \cdot 10^{-4}$M in CH_2Cl_2) in the presence of $Hg(OTf)_2$, carried out by UV/Vis analysis.

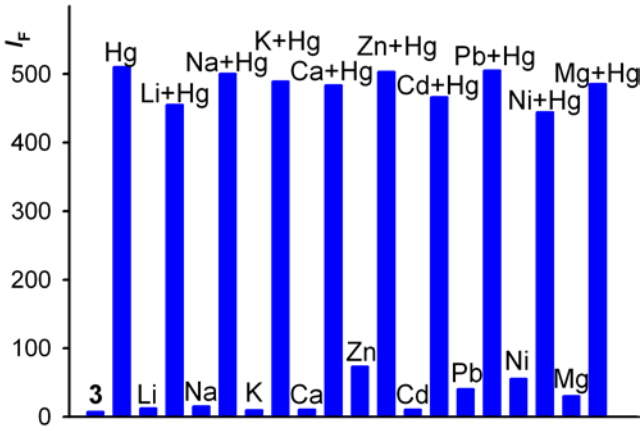

Figure S25. Fluorescence emission intensity of **3** upon addition of 0.5 equiv. of $Hg(OTf)_2$ in the presence of 1 equiv. of interference metal ions in CH_3CN/EtOH (7/3).

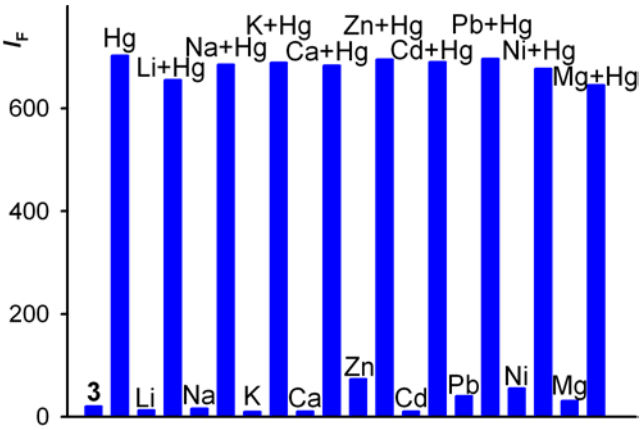

Figure S26. Fluorescence emission intensity of **3** upon addition of 0.5 equiv. of $Hg(OTf)_2$ in the presence of 1 equiv. of interference metal ions in CH_3CN/EtOH/H_2O (65/25/10).

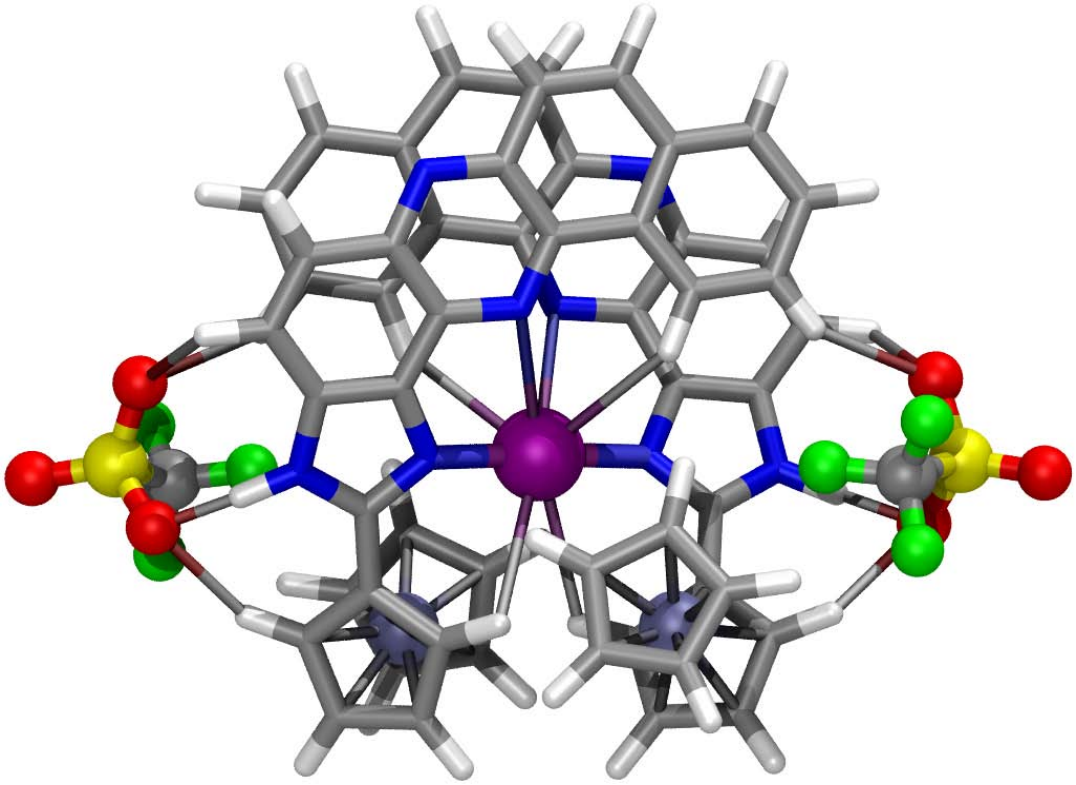

Figure S27. Calculated (vdw-RIJCOSX-B3LYP/def2-TZVP-ecp) structure for the most stable C_2-symmetric [**4**$_2$·Hg(TfO)$_2$] model complex.

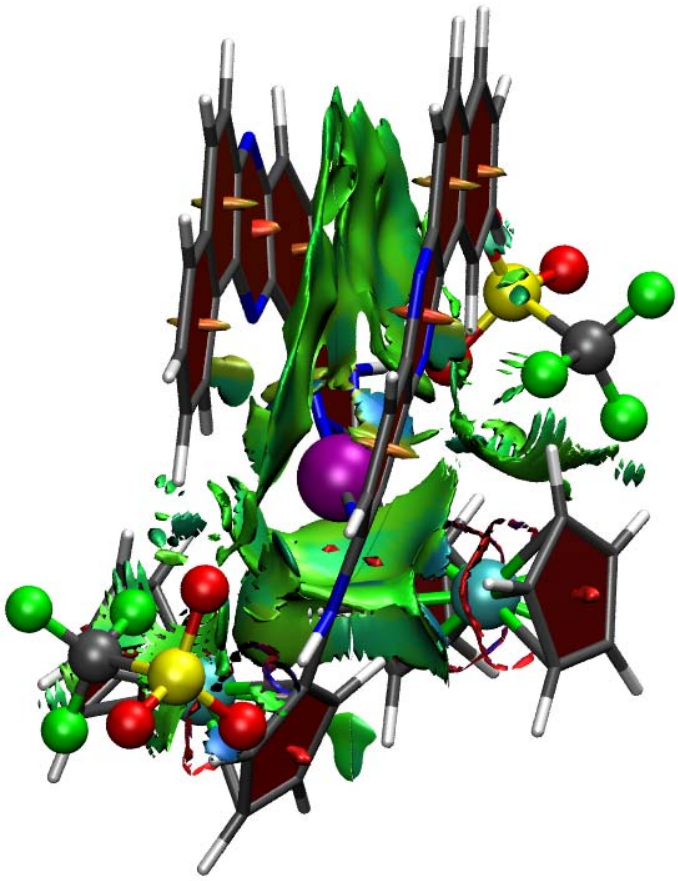

Figure S28. Side view for NCI isosurfaces in the calculated (vdw-RIJCOSX-B3LYP/def2-TZVP-ecp) structure for the most stable C_2-symmetric [**4**$_2$·Hg(TfO)$_2$] model complex highlighting π stacking

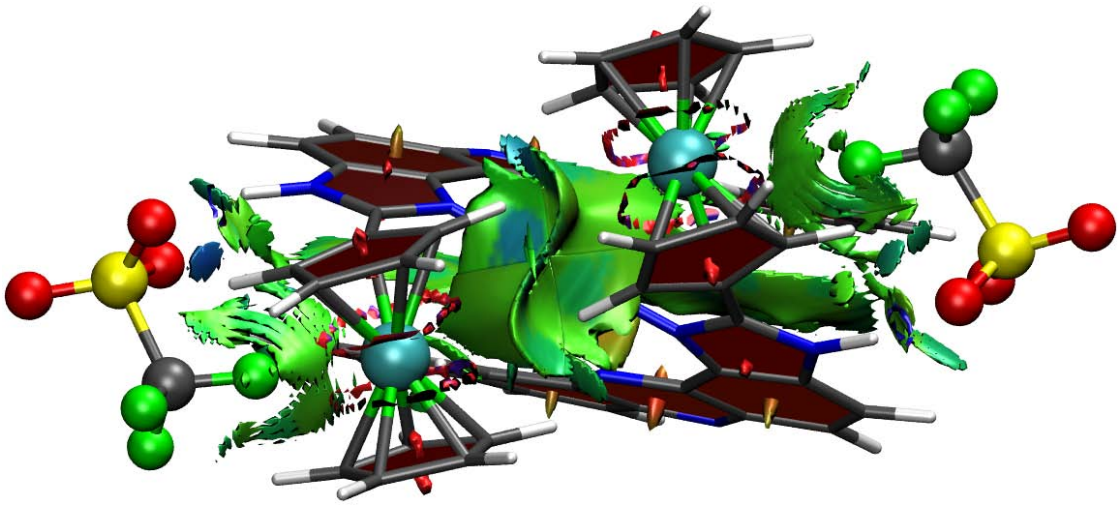

Figure S29. Front view for NCI isosurfaces in the calculated (vdw-RIJCOSX-B3LYP/def2-TZVP-ecp) structure for the most stable C_2-symmetric [**4**$_2$·Hg(TfO)$_2$] model complex highlighting hydrogen bonds with lateral anions and ferrocene interpenetration.

Calculated structures: cartesian coordinates (in Å) and energies for all computed species.-

Complex $\mathbf{4}_2 \cdot Hg(TfO)_2$ (C_2) E = -7120.815314304 au

E = -7119.82311389 au (RIJCOSX-B3LYP/def2-TZVP-f)

N	0.00000000	0.00000000	0.00000000	N	-4.15922451	-4.45784411	1.06732625
C	1.35141476	0.00000000	0.00000000	C	-4.65387109	-3.51196268	1.93872138
N	1.79873150	1.26068479	0.00000000	C	-3.67209301	-2.54851913	2.04174649
C	0.72303525	2.12092167	0.03957869	H	-4.68690163	-5.27759089	0.67028660
C	-0.39869055	1.31843798	0.01773885	C	-3.85547005	-1.36790571	2.78505622
H	2.81184609	1.52210922	0.11543182	C	-5.14399194	-1.19490187	3.38326358
C	-1.69871951	1.84395310	0.13496989	C	-6.12578312	-2.23519196	3.29569755
C	-1.78987518	3.25777532	0.33712925	C	-5.90252336	-3.38575296	2.59281837
C	-0.60842006	4.06842338	0.30886794	H	-7.07702379	-2.05143487	3.77649794
C	0.63808674	3.52854314	0.15911875	H	-6.66370263	-4.14148389	2.46489906
H	-0.74127986	5.13153652	0.45696662	N	-2.88978418	-0.44979276	2.85835693
H	1.53631158	4.12665210	0.20753635	C	-3.18062263	0.69367125	3.47504640
N	-2.76427732	1.04070714	0.11960604	C	-4.50814488	0.91658415	3.99284115
C	-3.95028721	1.59582944	0.35965317	N	-5.44534249	-0.03187997	3.96975851
C	-4.03986106	3.00277924	0.66393206	C	-2.18388085	1.73604469	3.59702292
N	-2.97702261	3.80673847	0.61412900	C	-0.84192166	1.54244355	3.22875580
C	-5.15226381	0.78950533	0.35673570	C	0.07636882	2.56593294	3.33051228
C	-5.15685929	-0.55505263	-0.05081715	C	-0.32445275	3.82195424	3.80557999
C	-6.31422890	-1.30356690	-0.01388109	C	-1.63085115	4.02987952	4.19557947
C	-7.50854264	-0.72495499	0.43640742	C	-2.57937293	2.99565645	4.11244760
C	-7.53463551	0.59967481	0.81940135	C	-3.92942977	3.19603708	4.55991521
C	-6.36861152	1.38373929	0.77635770	C	-4.84624056	2.20242765	4.52707233
C	-6.40242598	2.77500812	1.13168965	H	-0.53331332	0.57063755	2.87175258
C	-5.30133431	3.55666825	1.05762908	H	1.10316811	2.41780684	3.03345192
H	-4.23703138	-0.99612359	-0.40644383	H	0.40287307	4.62121508	3.86724092
H	-6.31108500	-2.34002242	-0.31430254	H	-1.94414826	4.99414551	4.57707815
H	-8.40711915	-1.32725311	0.47409097	H	-4.19423481	4.17384290	4.94404358
H	-8.45746581	1.05713171	1.15499431	H	-5.85936628	2.34116594	4.87960370
H	-7.35013826	3.19177023	1.45095644	C	-2.13352748	-4.82299317	-0.27267282
H	-5.32394903	4.60917924	1.30594258	C	-2.57714299	-5.79354678	-1.22527529
C	2.19694278	-1.16200656	-0.06613784	C	-1.42882922	-6.31439930	-1.87063505
C	3.56204043	-1.25128888	0.35190231	C	-0.27537498	-5.67718887	-1.33114213
C	4.00941215	-2.56570236	0.07158668	C	-0.70011970	-4.75475042	-0.34281401
C	2.93688372	-3.29598901	-0.51485222	H	-3.60372377	-6.05634102	-1.42038588
C	1.81311830	-2.43741986	-0.60487191	H	-1.43690708	-7.03544339	-2.67111298
H	4.12900340	-0.45986858	0.81364244	H	0.74359243	-5.84126714	-1.63875186
H	4.98433418	-2.95666701	0.31118727	H	-0.05389946	-4.15701386	0.27497606
H	2.96037019	-4.33088145	-0.81198190	Fe	-1.54215826	-4.26475702	-2.16989996
H	0.86633737	-2.68946873	-1.04830329	C	-2.57981421	-2.59297724	-2.84145257
Fe	2.39517869	-2.62840126	1.37303034	C	-1.18601771	-2.30023763	-2.76812249
C	1.49938573	-2.07643893	3.16619876	C	-0.49813231	-3.21460646	-3.61769801
C	0.86860404	-3.24675443	2.65023507	C	-1.46895111	-4.06065028	-4.22229846
C	1.85961177	-4.26335226	2.52586550	C	-2.75310647	-3.67872324	-3.74087559
C	3.09589917	-3.72263519	2.97646459	H	-3.36969782	-2.10053265	-2.29777884
C	2.87389757	-2.37226684	3.36878057	H	-0.72465938	-1.50763349	-2.20285250
H	1.03208108	-1.12293764	3.35183431	H	0.56974436	-3.26809427	-3.75633725
H	-0.17798521	-3.36625952	2.42446422	H	-1.26433468	-4.88084340	-4.89097716
H	1.70159510	-5.25633327	2.13668455	H	-3.68720408	-4.16345555	-3.97125935
H	4.04634648	-4.23093019	2.97507761	O	4.31192510	1.81832034	0.59176322
H	3.62529087	-1.67739850	3.70515319	S	4.30756233	2.67243370	1.80270180
Hg	-1.33791725	-1.41723581	0.62512973	O	3.09679348	3.47373446	1.91290380
N	-2.62278503	-2.89548608	1.21948484	O	5.56575269	3.28846290	2.12110958
C	-2.95785296	-4.06442994	0.62989044	C	4.04871007	1.37669678	3.12931159

F	3.99572113	1.90685369	4.35292683	O	-7.77259420	-6.66234337	-1.14291832
F	5.01411820	0.44022228	3.11540334	C	-6.18268309	-4.83438641	-2.19339218
F	2.87072840	0.72352658	2.91427056	F	-7.16195719	-4.17729353	-2.81817983
O	-5.52285881	-6.33763688	-0.19130946	F	-5.60594745	-5.67159728	-3.07409914
S	-6.78887382	-5.73063453	-0.66528737	F	-5.23182018	-3.91999723	-1.84659697
O	-7.22986373	-4.63217703	0.18271476				

Complex **4**$_2$·Hg(TfO)$_2$$^{no\text{-}interp.}$ (qC_2) E = -7119.81001123 au (RIJCOSX-B3LYP/def2-TZVP-f)

N	0.00000000	0.00000000	0.00000000	C	-4.61266965	-3.52006935	2.00839880
C	1.34621961	0.00000000	0.00000000	C	-3.64023806	-2.54676537	2.08788252
N	1.79110177	1.26469988	0.00000000	H	-4.65992125	-5.28944903	0.73411567
C	0.71003644	2.12183101	0.03646384	C	-3.82142301	-1.35769644	2.81833793
C	-0.40639084	1.31477278	0.01901114	C	-5.09895509	-1.19158019	3.43869248
H	2.80508181	1.50974321	0.12919743	C	-6.06524568	-2.24730737	3.38950002
C	-1.71035646	1.82083173	0.16065680	C	-5.84446215	-3.40198448	2.69548410
C	-1.81992778	3.22943024	0.36909915	H	-7.00850413	-2.07048333	3.88657244
C	-0.64812546	4.05172295	0.31998993	H	-6.60075708	-4.16514448	2.59335201
C	0.60325394	3.52849807	0.15639929	N	-2.86821352	-0.42484579	2.85448734
H	-0.78921152	5.11261465	0.47366182	C	-3.16426711	0.72592733	3.45487308
H	1.49100018	4.14085247	0.19770979	C	-4.48495129	0.93886531	3.99186763
N	-2.76006074	0.99779386	0.16932667	N	-5.40682961	-0.02288541	4.00639252
C	-3.94905689	1.53013188	0.44055606	C	-2.18050623	1.78276747	3.54494539
C	-4.05401592	2.93366120	0.75204968	C	-0.83797696	1.59857374	3.17502938
N	-3.00827134	3.75658592	0.67676983	C	0.06605034	2.63530437	3.25163263
C	-5.13421121	0.70168277	0.46584092	C	-0.35103000	3.89602519	3.69614740
C	-5.12754679	-0.63683589	0.04074285	C	-1.65703831	4.09589507	4.08627060
C	-6.26606950	-1.40899965	0.11246695	C	-2.58946085	3.04666899	4.03539574
C	-7.44997845	-0.86122896	0.62237381	C	-3.93432639	3.23653867	4.49880480
C	-7.48884455	0.45747346	1.02067633	C	-4.83355378	2.22865500	4.50601591
C	-6.34395182	1.26677459	0.93608400	H	-0.51272051	0.62333650	2.84324495
C	-6.39269896	2.65458398	1.29858266	H	1.09330995	2.49434723	2.95400934
C	-5.31303227	3.45939634	1.18670500	H	0.36534097	4.70598570	3.73575145
H	-4.21628802	-1.05427185	-0.36022192	H	-1.98230290	5.06333597	4.44816869
H	-6.25499071	-2.44130276	-0.20303217	H	-4.20753089	4.21801520	4.86642808
H	-8.33189950	-1.48440158	0.69340610	H	-5.84150820	2.35829096	4.87457482
H	-8.40562848	0.89102001	1.40047380	C	-2.13845205	-4.75065694	-0.31513115
H	-7.33577914	3.04965008	1.65585042	C	-0.70080555	-4.74259671	-0.35087912
H	-5.34951740	4.50950185	1.44175467	C	-0.29420932	-5.63647868	-1.37430705
C	2.15619571	-1.19150590	-0.02674388	C	-1.46086191	-6.19858645	-1.96542297
C	1.81256210	-2.40088384	-0.72329727	C	-2.60127317	-5.66565699	-1.31667664
C	2.88177426	-3.31521327	-0.54600576	H	-0.04384590	-4.20882318	0.31547944
C	3.88090778	-2.68422944	0.24860890	H	0.72463406	-5.88111204	-1.62391071
C	3.44864686	-1.37287942	0.56636093	H	-1.47936739	-6.94168462	-2.74465206
H	0.93353210	-2.56352635	-1.32364739	H	-3.62688644	-5.92694701	-1.50064764
H	2.94393478	-4.29819961	-0.98184928	Fe	-1.43141127	-6.61659369	0.06797347
H	4.83131577	-3.10925415	0.52422877	C	-2.06382767	-7.09018099	1.96374129
H	3.99628864	-0.62690107	1.11104080	C	-2.69021037	-7.94269334	1.01113780
Fe	3.54045100	-1.57300668	-1.46784608	C	-1.66323037	-8.65084331	0.32551872
C	3.52377509	0.02521946	-2.76421201	C	-0.40738116	-8.23464946	0.85044298
C	4.78185987	-0.05896597	-2.10517590	C	-0.65541901	-7.26898436	1.86663578
C	5.35099971	-1.32454779	-2.42145344	H	-2.56968629	-6.38517498	2.60363940
C	4.44517779	-2.02112873	-3.27010007	H	-3.74643891	-7.98444182	0.79599775
C	3.31335461	-1.18485356	-3.48341506	H	-1.81200208	-9.34423740	-0.48591153
H	2.82655934	0.84386441	-2.68369324	H	0.56063120	-8.56565327	0.51325307
H	5.18762547	0.67543107	-1.42779392	H	0.09188042	-6.73711419	2.43141922
H	6.28335445	-1.70825840	-2.04193072	O	4.32419797	1.71517305	0.68241424
H	4.57586247	-3.02022743	-3.65190460	S	4.24271762	2.53320817	1.91620094
H	2.43701580	-1.43770683	-4.05778001	O	3.06894544	3.39278555	1.92530538
Hg	-1.32118187	-1.42741984	0.62176127	O	5.49164505	3.07421233	2.37014251
N	-2.61371349	-2.88296901	1.23284172	C	3.79086653	1.24202239	3.19066507
C	-2.95185690	-4.04574283	0.64261562	F	3.60855865	1.78403811	4.39520502
N	-4.13988891	-4.45243351	1.11070312	F	4.72915062	0.28971603	3.28668274

F	2.63042484	0.62572330	2.83773620
O	-5.49316674	-6.39864984	-0.05429921
S	-6.75623022	-5.78873913	-0.53874612
O	-7.18067069	-4.67347836	0.29313649
O	-7.74553609	-6.72744175	-0.98434068
C	-6.17502311	-4.92431922	-2.08730020
F	-7.17143878	-4.28484777	-2.69811918
F	-5.62060898	-5.78277224	-2.95522923
F	-5.22508037	-4.00404696	-1.77013